Modelling and assessing the near-wake representation and turbulence behaviour of control-oriented wake models

Paul Hulsman[1], Luis A. Martínez-Tossas[2], Nicholas Hamilton[2], and Martin Kühn[1]

[1] ForWind – University of Oldenburg, Institute of Physics, Küpkersweg 70, 26129 Oldenburg, Germany
[2] National Wind Technology Center, National Renewable Energy Laboratory, Golden, CO, 80401, USA

E-mail: paul.hulsman@forwind.de

Abstract. Due to the interaction between the wake of an upstream turbine on a downstream turbine, power losses and increased fatigue loads occur. By yawing the upstream turbine with regard to the wind direction, one can potentially reduce the power losses of the downstream turbine and reduce the fatigue loads. The evolution of the wake depends on the pressure gradient within the near-wake region and the turbulent kinetic energy and must be incorporated in existing wake steering algorithms to provide an accurate estimation of the wake flow. This paper will show a first approach to implement a near-wake model and a turbulence model in the curled wake model within the controls-oriented framework FLORIS. The near-wake model is based on an analytical expression of the velocity profile to model the pressure gradient. Furthermore, two turbulence models are incorporated within the curled wake model based on a Gaussian-distribution and a mixing length formulation. The adapted curled wake model is then assessed with the measurement data acquired in the wind tunnel at ForWind – University of Oldenburg. The evaluation of the models show good agreement for the velocity deficit and representation of the near-wake region. Furthermore, the turbulent kinetic energy behaved as expected in comparison to other work, showing a ring of high turbulent kinetic energy at non-yawed condition which is deflected to a curled shape at large yaw angles with the turbulence model based on a mixing length formulation.

1. Introduction

Wind turbines operating in the wake of upstream turbines experience power losses within a wind farm. Currently, one of the techniques used to reduce the wake interaction between turbines within a wind farm is to yaw an upstream turbine with regard to the incident wind direction. The objective is to deflect the wake such that downstream turbines can produce more power. This can potentially increase the overall power output and the annual energy production of the wind farm [1, 2]. The spacing between the

turbines can be as low as 3 rotor diameters (D) [3, 4], indicating that wind turbines can operate in the near-wake region of upstream turbines, depending on plant design and atmospheric conditions. The development of downstream wakes is related to the turbulence kinetic energy (TKE) within the wake, defining the dissipation and the mixing of the wake with the ambient air. This underpins the importance of modeling near-wake aerodynamics and the TKE while redirecting the wake in order to implement wake steering algorithms at existing wind farms. In this work, we implement a near-wake model and a model for the TKE within the curled wake model to provide a better prediction of the velocity deficit and the turbulence intensity (TI) in the near wake. Realistic representation of the near-wake will also inherently produce a better assessment of the power production.

The first analytical model for the velocity deficit in a wind turbine wake was developed by [5] and subsequently advanced by [6] and [7]. These models are based on the conservation of mass and momentum and have either a top-hat distribution or a Gaussian distribution of velocity. Another approach to model the wake profile is by using the Prandtl turbulent boundary equations [8, 9], or other simplified forms of the Navier-Stokes equations [10] and more recently in the curled wake model [11]. These models give a good approximation of the far wake as the velocity deficit is well represented by a single-Gaussian distribution. However, in the near-wake the velocity follows a double-Gaussian distribution [12, 13]. The wake profile within the near-wake is modeled using a Gaussian near-wake approach to model the wake profile by [14] and using the momentum theory and the blade element theory by [15]. More recently, the near wake was modeled by [16] based on the conservation of mass and momentum assuming a double-Gaussian distribution of the wake. The turbulent kinetic energy quantifies the magnitude and importance of stochastic fluctuations of the velocity field and is commonly used to analyze the evolution and decay of wakes [17, 18]. Schottler [17] showed that a ring of high turbulence kinetic energy, slightly larger than the rotor area, is formed directly behind the turbine, where it was observed that the turbulence level decreased and is deflected for large yaw angles with respect to the incoming flow. Given these observations, TKE must be taken into account in engineering models in order to improve the prediction of wake development [18] and provide a prediction of the loads on the downstream turbine and thus their lifetimes [19].

The aim of this research is to model and assess the near-wake region of a wake from a yawed wind turbine with existing control-oriented wake models. The implementation will be conducted by incorporating the near-wake model based on [16] into the curled wake model within FLORIS (**FLO**w **R**edirection and **I**nduction in **S**teady State). FLORIS is a controls-oriented framework used to test engineering wake models [20], which at the time of this study did not include a near wake model. Subsequent development in the FLORIS framework has introduced near-wake modeling capability. In addition, a simplified model to estimate the turbulence kinetic energy is introduced and implemented within the curled wake model. The method to incorporate the near-wake model is detailed in Section 2.1, followed by the implementation of the model for the TKE in Section 2.2. The setup of the measurement campaign is described in Section 2.3. The data acquired from the measurement campaign are then used to assess the behaviour of the new wake model in Section 3.

2. Methodology

2.1. Incorporating the near-wake model

Computationally-efficient modelling of the wake is a challenging problem due to the complex nature of the flow. The main aim of most engineering wake models is to predict the velocity deficit and the level of TI. In order to solve for these physical quantities, most wake models are based on a simplified version of the Reynolds-averaged Navier-Stokes equation, shown in Equation 1, as it is computationally expensive to solve it directly. Here $\overline{u}$ is the time-averaged streamwise velocity component, $\overline{v}$ is the time-averaged spanwise velocity component and $\overline{w}$ is the time-averaged wall-normal velocity component. Furthermore, $\overline{p}$ is the time-averaged pressure, ρ is the density and ν_{eff} is the effective viscosity. The first part of the equation (I) accounts for the transport of momentum due to convection. The second part of the equation (II) takes into account the pressure gradient and is significant in the near-wake but negligible in the far-wake. The third term (III) represents the combination of turbulent and molecular diffusion.

$$\underbrace{\overline{u}\frac{\partial \overline{u}}{\partial x} + \overline{v}\frac{\partial \overline{u}}{\partial y} + \overline{w}\frac{\partial \overline{u}}{\partial z}}_{I} = \underbrace{-\frac{1}{\rho}\frac{\partial \overline{p}}{\partial x}}_{II} + \underbrace{\nu_{\text{eff}}\left(\frac{\partial^2 \overline{u}}{\partial x^2} + \frac{\partial^2 \overline{u}}{\partial y^2} + \frac{\partial^2 \overline{u}}{\partial z^2}\right)}_{III} \tag{1}$$

The curled wake model, developed by [11], solves the linearized version of the Reynolds-averaged Navier–Stokes momentum equation for an incompressible flow, with the assumption that the pressure gradient can be neglected. As already mentioned, this is valid for the far-wake but not for the near-wake, since the wake deficit within the near-wake is heavily influenced by the pressure gradient. Furthermore, within the curled wake model the Reynolds-averaged Navier–Stokes momentum equation is solved as a marching problem starting from an initial condition at the rotor and moving downstream [11]. An analytical expression for the velocity profile within the near-wake region from the model proposed by Keant et al. [16] is used to make a first order approximation of the pressure gradient

$$\frac{\partial \overline{p}}{\partial x} = \frac{1}{2}(U(x_n)^2 - U(x_{n-1})^2)/dx \tag{2}$$

within the marching problem in order to improve the original formulation of the curled wake model. The equation for the velocity within the wake (U) is shown below, with U_∞ for the free-stream velocity σ for the cross-section width of a single Gaussian distribution, c is a pre-defined function, f, a tuning coefficient κ, and r_0 is the radial location of the Gaussian minimum [16].

$$U(x) = U_\infty \left(1 - \kappa\, c(x) f(r, \sigma(x))\right) \tag{3}$$

2.2. Simplified wake turbulence model

Two methods are used to incorporate the TKE within the curled wake model. The first approach is using the turbulence model introduced by [21], which estimates the local TI within the wake. The model will be used to estimate the effective viscosity ($\nu_{\text{eff}} = \nu_{\text{T}} + \nu$), shown in Equation (4) [22]. The effective viscosity is the summation of the turbulent viscosity (ν_{T}) and the kinematic viscosity (ν). Here $C_\mu = 0.09$ is a

constant, k is the turbulent kinetic energy and ε is the energy dissipation rate. The TKE is defined as the trace of the Reynolds stress tensor, represented as the matrix of covariance of velocity fluctuations. It is calculated from the averaged perturbations of the three velocity components (u, v, w) at a certain point in space with the following formulation: $k = \frac{1}{2}(\overline{u'^2} + \overline{v'^2} + \overline{w'^2})$. Here, u is the stream-wise velocity component and $u'(t)$ is the fluctuation of the flow, defined as $u'(t) = u(t) - \overline{u(t)}$. Furthermore, [23] showed a degree of isotropy of the standard deviation in the wake, $\overline{u'^2} = \overline{v'^2} = \overline{w'^2}$, which simplifies the relationship between the TKE and the TI (here I) to $k = \frac{3}{2}(\overline{u'^2})$ with $\overline{u'^2} = (U_h I)^2$. This assumption is not fully valid in a wind turbine wake [24, 25, 26], but is used to give a first-order of approximation of the turbulence. Because ε cannot be easily computed, a transfer function is used to estimate the energy dissipation rate from the TI fitted with the measurement data obtained from [27].

$$\nu_\mathrm{T} = C_\mu \frac{k^2}{\varepsilon} \tag{4}$$

The second approach uses a mixing length formulation introduced by [28], which relates the local turbulence on the length scale and the local strain rate tensor [29]. The mixing length model uses a single characteristic length scale at each downstream location, shown in Equation (5). Here F_1 is a filter function to model the reduction of wake dissipation due to the entrainment and F_2 is a filter function to account for non-equilibrium between the averaged velocity field and the turbulent flow due to the large velocity gradients over the rotor area. c_amb and c_2 are constants of the model and $\frac{\delta u}{\delta r}$ is the axial velocity gradient in radial direction. I_amb and U_h are the ambient TI and the free stream velocity at hub height. The turbulence length scale (l_*^2) is assumed to be half of the wake width [28]. TKE is calculated from the turbulent viscosity using the approximation from [30] for the length scale resulting in $k = (\frac{\nu_\mathrm{T}}{0.16R})^2$

$$\nu_\mathrm{T} = F_1 c_\mathrm{amb} I_\mathrm{amb} + F_2 c_2 l_*^2 \frac{\delta u}{\delta r} (\frac{1}{0.5 D\, U_\mathrm{h}}) \tag{5}$$

2.3. Wind tunnel measurements

Measurement data from [27] and [31] are used to evaluate the implementation of the near wake model and the turbulence model. Both measurement campaigns had the same layout and inflow condition but used different measurement systems to capture the flow behaviour. The measurements performed in [31] used a short-range Lidar WindScanner to obtain high spatial and temporal resolution observations of a model turbine from 1 D to 5 D. An array of hot-wires is used in [27] to measure the flow structures of an non-yawed turbine. Both measurement campaigns were conducted using the MoWiTO 0.6 (**Mo**del **Wi**nd **T**urbine **O**ldenburg), with a hub height of 0.77 m and a rotor diameter of $D = 0.58\,m$, in the large wind tunnel at ForWind – University of Oldenburg, which has the dimensions of 3 m by 3 m for the nozzle and is not fitted with a grid at the test section entrance to further alter the inflow condition. This resulted in a uniform inflow of $7.5\frac{m}{s}$ with a TI of 0.3 %. Furthermore, the turbine is yawed at $\psi = -30°$, 0°, 30° during the measurement campaign with the Lidar WindScanner [31], with a clockwise rotation viewed from above defined as a negative yaw angle. The WindScanner

performed multiple vertical scans (3 D by 3 D) at multiple downstream distances behind the wind turbine model providing a three dimensional representation of the evolution of the streamwise velocity component behind the wind turbine. The streamwise velocity component is extracted from the line-of-sight velocity with the assumption that the lateral and vertical velocity components are negligible, after which it is collocated onto a grid of 7 cm by 7 cm. The measurements conducted with the hot-wire [27] will be used to evaluate the near wake model and tune the near-wake model and the turbulence model. The data acquired with the WindScanner [31] will be used to analyze the wake characteristics of the yawed turbine.

3. Results

3.1. Near-wake region

The initial result of the implementation of the near-wake model, including the modelling of the effective viscosity, is shown in Figure 1. The figure indicates the comparison between the mean flow at the center line of the experimental hot-wire data [27] and the curled wake model with and without the implementation of the near-wake model and the turbulence model at $\psi = 0°$. The shortcomings of the current version of the curled wake model is clearly visible as it can not predict the velocity deficit within the near wake region, thus leading to an over-prediction of the velocity component until it corresponds at 10 D. Incorporating the near-wake model leads to a better estimate of the velocity deficit, indicating a speed-up region between 1 D to 5 D. The turbulence model introduced by [28] provides a more accurate result for the velocity deficit within the near-wake region due to the filter function F_1, which accounts for the deceleration and expansion due to the pressure field and avoids nonphysical turbulence diffusion.

With the implementation of the near-wake model and the two different turbulence models, the outcome of the curled wake model (blue line and red line) is shown in Figure 2. The curled wake model follows a double-peak Gaussian distribution of the near-wake at $\psi = 0°$ for both turbulence models, which slowly develops into a single Gaussian distribution in the far-wake shown in Figure 2. The difference between the experimental

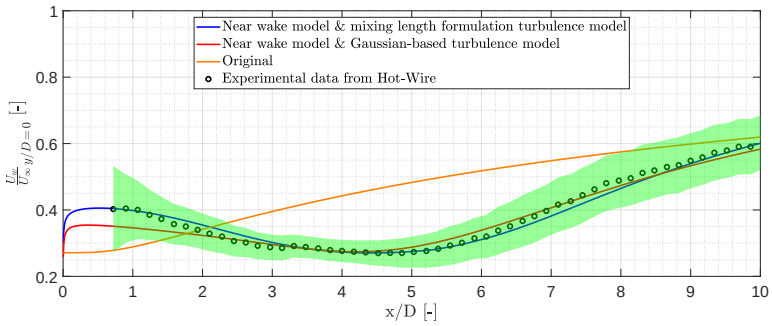

Figure 1: Comparison of the streamwise velocity component at the rotor center for each downstream distance acquired with the original curled wake model, the adapted curled wake model with the turbulence models and the hot-wire measurements [27]. The shaded area indicates $\pm\sigma$ of the hot-wire measurements

data from the WindScanner [31] and the hot-wire [27] is due to spatial averaging by the lidar and the procedural differences in the measurements. The development of the wake matches the development of the experimental data [27] (black circles). The curled wake model without any modifications (orange line) has a good agreement with the experimental data in the far-wake. However, within the near-wake, the curled wake model and the experimental data differ and do not follow a double-peak Gaussian distribution throughout the entire domain. The width of the velocity deficit profile is slightly smaller in the case with the Gaussian-based turbulence model at 3 D and at 5 D, due to the difference in viscosity.

For the case with $\psi = -30°$ (Figure 2a), the modified curled wake model shows a better agreement with the WindScanner data at 1 D in comparison to the original curled wake model. However, a difference is noticeable between the position with the lowest velocity obtained by the adapted curled wake models and the experimental data. This is due to the fact that the shift of the center of the counter-rotating vortex pair is not accounted for in the current version of the curled wake model. A similar behaviour is

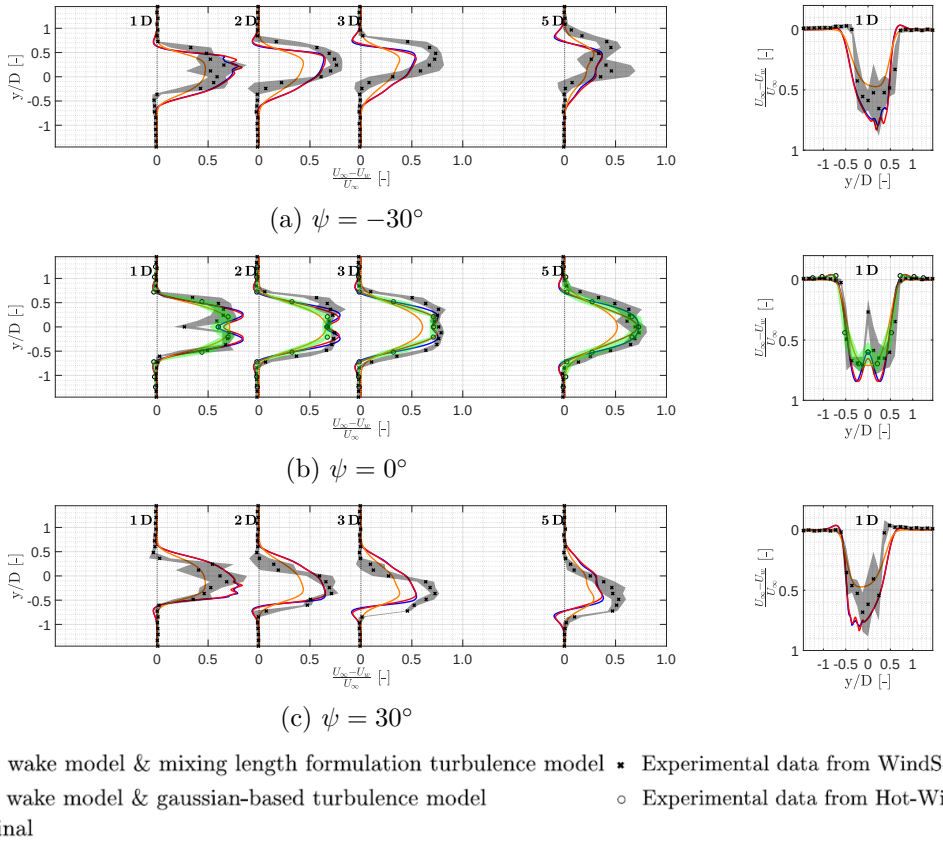

(a) $\psi = -30°$

(b) $\psi = 0°$

(c) $\psi = 30°$

Figure 2: Comparison of the mean wake flow ($\frac{U_\infty - U_w}{U_\infty}$ [$\frac{m}{s}$]) at hub height between the experimental data and the curled wake model. The shaded area indicates the $\pm\sigma$ of each measurement case. **Green**: Hot-wire measurements **Grey**: WindScanner data

observed at $\psi = 30°$ (Figure 2c). Furthermore, the velocity profiles estimated with both turbulence models are very similar.

Due to the implementation of the near-wake model to account for the pressure gradient, the speed-up region at the edges of the wake ($\frac{y}{D} \approx \pm 0.6$) is also visible at $\psi = -30°$ (Figure 2a), $\psi = 0°$ (Figure 2b) and $\psi = 30°$ (Figure 2c). At $\psi = 0°$ the speed-up region regions remains visible at a downstream distance up to $7\,D$, after which it diminishes. As expected, the speed-up region becomes less significant moving further downstream due to the reduction of the pressure gradient. However, this indicates that the pressure gradient in the modified curled wake model decays slowly, until it has recovered compared to the experimental hot-wire data [27]. This can be accounted for by further tuning the model. At $\psi = \pm 30°$ a similar phenomena is visible, showing the presence of the speed-up region until $7\,D$ after which it decays.

3.2. Turbulence kinetic energy

The implementation of the turbulence model within the curled wake model is evaluated by comparing the viscosity and the TKE with the data obtained by the hot-wire measurements [27]. The TKE is estimated with $k = \frac{3}{2}(\overline{u'^2})$ for the Gaussian-based turbulence model [21] within the curled wake model and the measurement data. Since the turbulence model is based on the mixing length [28] it only provides an effective viscosity, the following approximation is used to arrive at an estimate of TKE: $k = (\frac{\nu_T}{0.16R})$. The approximation is based on the characteristic length scales in wakes [30] and assumes that the turbulent stresses are based on the local ratio of dissipation and turbulence production. However, this approach is valid when the eddy viscosity distribution within the wake is uniform over the rotor area which occurs at a large downstream distance [28].

Figure 3 indicates the comparison between the effective viscosity and the TKE computed with the hot-wire measurement data [27] and with the two different turbulence models at $7\,D$. The distribution of the viscosity (Figure 3a) estimated by the turbulence models are on the same order of magnitude and have a similar distribution as the measurement data. In addition, a difference is noticeable in the viscosity between the

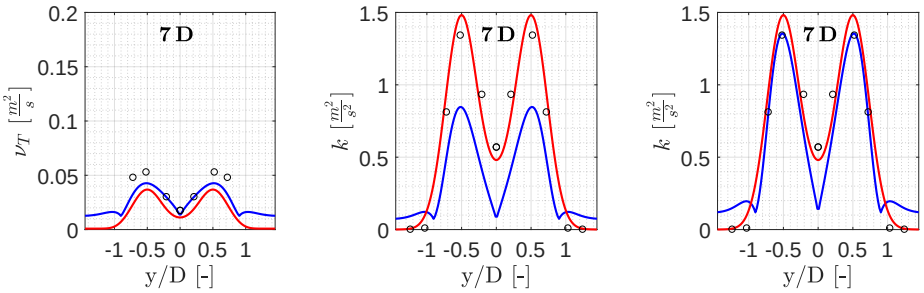

(a) ν_T (b) $k = (\frac{\nu_T}{0.16R})^2$ (c) $k = (\frac{\nu_T}{0.13R})^2$

Figure 3: Profile of the viscosity (a), the TKE with a characteristic length scale of 0.16R (b) and 0.13R (c) in comparison to the hot-wire measurement data [27]. **Blue**: Mixing-length formulation turbulence model **Red**: Gaussian-based turbulence model

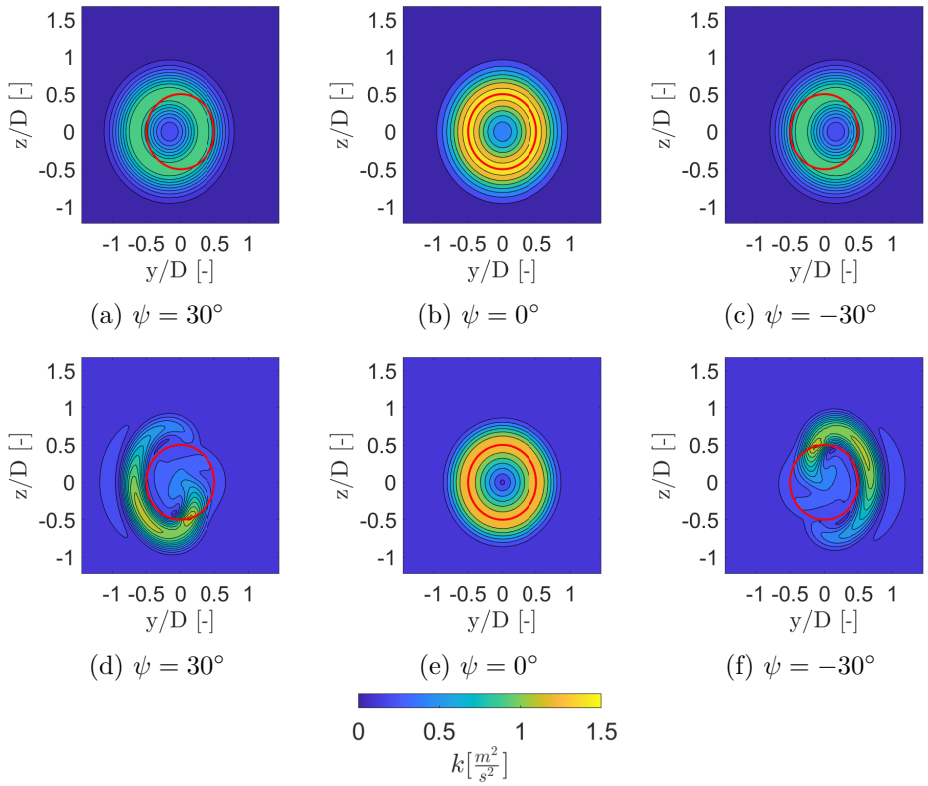

Figure 4: Comparison of the TKE at 7 D estimated by the Gaussian-based turbulence model (a to c) and the mixing length formulation turbulence model (d to f), estimated with $k = (\frac{\nu_T}{0.13R})^2$, at different operational conditions.

different models; the turbulence model based on a mixing length formulation accounts for the viscosity due to the ambient turbulence, seen in Equation (5). The TKE computed by the turbulence models is shown in Figure 3b and in Figure 3c. The figures show a clear correlation between the TKE modelled by the Gaussian-based turbulence model and the measurement data. Moreover, a discrepancy is visible between the measurement data and the turbulence model based on a mixing length formulation, which is attributed to the use of the characteristic length scale. Figure 3c shows the profile of the TKE with a characteristic length scale of $0.13R$. However, both turbulence models indicate the same distribution of the TKE within the wake. Since the turbulence model based on the mixing length is computed through the velocity gradient, a lower TKE is obtained at the wake center. This is due to the small magnitude of the velocity gradient at the wake center.

The TKE obtained from the Gaussian-based turbulence model is shown in Figure 4a - 4c. At $\psi = 0°$ (Figure 4b), a ring of high TKE is visible of the same size as the rotor diameter [32, 18, 17], with the highest TKE visible at the edge of the wake due to the shear layer between the ambient flow and the wake. At $\psi = \pm 30°$ the ring is shifted

based on the wake deflection [33], maintaining the circular shape with a reduced intensity of the TKE. The Gaussian-based turbulence model estimates the turbulence with the thrust coefficient. As the thrust reduces at a large yaw angle, the estimated turbulence is reduced as well [18].

At $\psi = 0°$, the TKE computed with the mixing length turbulence model shows similar behaviour as the TKE computed with the Gaussian-Based turbulence model, indicating a ring of high turbulence energy with the same size as the rotor diameter. Similar behaviour is observed for the TKE obtained with the turbulence model based on a mixing length formulation within the curled wake model, indicating a ring of high turbulence energy with the same size as the rotor diameter. For the curled wake model, the TKE is deflected *and* deformed to a curled shape accordingly at large yaw angles. This corresponds with other studies analyzing the behaviour of the TKE at large yaw angles [32, 18, 17]. In addition, the magnitude of the TKE is also reduced at $\psi = \pm 30°$.

4. Conclusion

In this study the implementation of a near-wake model and a simplified turbulence model within the curled wake model is introduced and assessed. The implementation of the near-wake model is conducted by using the model developed by [16] and shows promising results to determine the wake deficit and wake shape close to the turbine. The velocity deficit acquired from the hot-wire measurement data [27] shows good agreement with the velocity deficit estimated by the modified curled wake model. A double Gaussian distribution is seen close to the turbine, which slowly diminishes further downstream. The speed-up region is also introduced by the near-wake model due to the approximation of the pressure gradient. This phenomenon was not captured by the original formulation of the curled wake model and corresponds with the data from [31].

Two turbulence models are implemented within the curled wake model, assessed against each other and with the measurement data. The first turbulence model is based on a Gaussian distribution of the turbulence for the prediction of the velocity perturbations [21]. The turbulence model calculates a ring of high turbulence at $\psi = 0°$, which shifts at $\psi = \pm 30°$ accordingly and reduces in magnitude. The ring of high turbulence is not deflected and deformed into a curled shape, observed in [17] as it is based on a Gaussian distribution. The second turbulence model, based on a mixing length formulation, shows the deformation of the ring of high turbulence at a large yaw angle. This highlights the advantage of the second turbulence model. In addition, the magnitude of the TKE is also reduced at $\psi = \pm 30°$. A difference in the magnitude of the TKE is observed between both models, which is attributed to the use of the characteristic length scale to estimate the TKE. The distributions of viscosity and TKE show a good agreement with the hot-wire measurement data [27].

The modified curled wake model improves the prediction of wake velocity evolution which will be of benefit in future predictions of structural loads on downstream turbines and, thus, estimates of their lifetimes. In order to further enhance the integration of the near wake model and the simplified turbulence models, results need to be reevaluated for different inflow conditions and through the use of experimental data and high-fidelity simulations. In addition, the estimate for the pressure gradient needs to be further expanded to account for the asymmetry of the wake.

Acknowledgments
This work is partly funded by the Federal Ministry for Economic Affairs and Energy according to a resolution by the German Federal Parliament in the scope of research project "CompactWind II" (Ref. Nr. 0325492H).

References

[1] Fleming P, King J, Dykes K, Simley E, Roadman J, Scholbrock A, Murphy P, Lundquist J K, Moriarty P, Fleming K, van Dam J, Bay C, Mudafort R, Lopez H, Skopek J, Scott M, Ryan B, Guernsey C and Brake D 2019 *Wind Energy Science* **4** NREL/JA–5000–73991
[2] Howland M F, Lele S K and Dabiri J O 2019 *Proceedings of the National Academy of Sciences* **116** 14495–14500
[3] Hamilton N 2019 Total variation of atmospheric data: covariance minimization about objective functions to detect conditions of interest Tech. rep. National Renewable Energy Lab.(NREL), Golden, CO (United States)
[4] Nilsson K, Ivanell S, Hansen K S, Mikkelsen R, Sørensen J N, Breton S P and Henningson D 2015 *Wind Energy* **18** 449–467
[5] Jensen N O 1983 *Risø National Laboratory*
[6] Frandsen S, Barthelmie R, Pryor S, Rathmann O, Larsen S, Højstrup J and Thøgersen M 2006 *Wind Energy: An International Journal for Progress and Applications in Wind Power Conversion Technology* **9** 39–53
[7] Bastankhah M and Porté-Agel F 2014 *Renewable Energy* **70** 116–123
[8] Larsen G C, Højstrup J and Madsen H A 1996 *EWEC 1996 Proceedings, Goteborg (Sweden)*
[9] Larsen G C 1988 *A simple wake calculation procedure* (Risø National Laboratory)
[10] Crespo A, Hernandez J, Fraga E and Andreu C 1988 *Journal of Wind Engineering and Industrial Aerodynamics* **27** 77–88
[11] Martínez-Tossas L A, Annoni J, Fleming P A and Churchfield M J 2019 *Wind Energy Science (Online)* **4**
[12] Vermeer L, Sørensen J N and Crespo A 2003 *Progress in aerospace sciences* **39** 467–510
[13] Aitken M L, Banta R M, Pichugina Y L and Lundquist J K 2014 *Journal of Atmospheric and Oceanic Technology* **31** 765–787
[14] Ainslie J F 1988 *Journal of Wind Engineering and Industrial Aerodynamics* **27** 213–224
[15] Magnusson M 1999 *Journal of Wind Engineering and Industrial Aerodynamics* **80** 147–167
[16] Keane A, Aguirre P E O, Ferchland H, Clive P and Gallacher D 2016 An analytical model for a full wind turbine wake *Journal of Physics: Conference Series* vol 753 p 032039
[17] Schottler J, Bartl J M S, Mühle F V, Sætran L R, Peinke J and Hölling M 2018 *Wind Energy Science* **3** 257–273
[18] Bartl J M S, Mühle F V, Schottler J, Sætran L R, Peinke J, Adaramola M S and Holling M 2018 *Copernicus Publications*
[19] Burton T, Jenkins N, Sharpe D and Bossanyi E 2001 *Wind energy handbook* vol 2 (Wiley Online Library)
[20] Annoni J, Fleming P, Scholbrock A, Roadman J, Dana S, Adcock C, Porte-Agel F, Raach S, Haizmann F and Schlipf D 2018 *Wind Energy Science* **3** NREL/JA–5000–72767
[21] Ishihara T and Qian G W 2018 *Journal of Wind Engineering and Industrial Aerodynamics* **177** 275–292
[22] Launder B and Spalding D 1974 *Elsevier* **3** 269–289
[23] Larsen G C, Madsen H A, Larsen T J and Troldborg N 2008 *Forskningscenter Risoe Roskilde, Tech. Rep*
[24] Hamilton N and Cal R B 2015 *Physics of Fluids* **27** 015102
[25] Hamilton N, Tutkun M and Cal R B 2017 *Physical Review Fluids* **2** 014601
[26] Ali N, Hamilton N, Cortina G, Calaf M and Cal R B 2018 *Journal of Renewable and Sustainable Energy* **10** 013301
[27] Neunaber I 2019 Ph.D. thesis University of Oldenburg

[28] Keck R E, Veldkamp D, Wedel-Heinen J J and Forsberg J 2013 Ph.D. thesis
[29] Pope S B 2001 *Turbulent flows* (Cambridge University Press)
[30] Versteeg H K and Malalasekera W 2007 *An introduction to computational fluid dynamics: the finite volume method* (Pearson education)
[31] Hulsman P, Wosnik M, Petrović V, Hölling M and Kühn M 2020 Turbine wake deflection measurement in a wind tunnel with a lidar windscanner *Journal of Physics: Conference Series* vol 1452 p 012007
[32] Eriksen P E and Krogstad P Å 2017 *Renewable Energy* **108** 449–460
[33] Qian G W and Ishihara T 2018 *Energies*